Available online at www.sciencedirect.com
SCIENCE DIRECT®
European Journal of Medicinal Chemistry 38 (2003) 351–356
EUROPEAN JOURNAL OF MEDICINAL CHEMISTRY
www.elsevier.com/locate/ejmech

Lipopeptide substrates for SpsB, the *Staphylococcus aureus* type I signal peptidase: design, conformation and conversion to α-ketoamide inhibitors

Gordon Bruton [a,*], Anthony Huxley [a], Peter O'Hanlon [a], Barry Orlek [a], Drake Eggleston [b], John Humphries [a,1], Simon Readshaw [a], Andrew West [a], Stephen Ashman [a], Murray Brown [c], Keith Moore [c], Andrew Pope [d], Karen O'Dwyer [e], Lei Wang [e,2]

[a] *GlaxoSmithKline, New Frontiers Science Park, Harlow, Essex CM19 5AW, UK*
[b] *GlaxoSmithKline, Research Triangle Park, P.O. Box 13398, NC 27709, USA*
[c] *GlaxoSmithKline, Stevenage, Hertfordshire SG1 2NY, UK*
[d] *GlaxoSmithKline, King of Prussia, PA 19406, USA*
[e] *GlaxoSmithKline, P.O. Box 5089, Collegeville, PA 19426-0989, USA*

Received 27 September 2002; received in revised form 18 December 2002; accepted 23 January 2003

Abstract

Pre-protein sequence data was used to design substrates for SpsB, the bacterial signal peptidase I enzyme from *Staphylococcus aureus*. Key elements were an alkyl membrane anchor, proline at P5 and lysine at P2. The proline at P5 induced a helical turn in the lipopeptide, as deduced from NMR studies, from P6 to P2 in membrane mimetic solvents. The substrate Decanoyl-LTPTAKAASKIDD-OH was cleaved by SpsB, as expected, between the P1 and P1′ alanines with a k_{cat}/K_m of 2.3×10^6 $M^{-1} s^{-1}$ at pH 8.5. Insertion of proline at P1′ converted substrates to competitive inhibitors, whilst the incorporation of an α-ketoamide at the cleavage site transformed substrates to time dependent inhibitors of SpsB.

Keywords: *S. aureus*; SpsB; Signal peptidase; Substrate; Inhibitor; Lipopetide

1. Introduction

Signal peptidase I enzymes (SPases) are broad-spectrum antibacterial targets essential for growth [1,2]. As serine proteases they cleave N-terminal signal sequences from pre-proteins, thus liberating mature proteins from the bacterial cytoplasmic membrane. The pre-protein cleavage site is defined by Ala–X–Ala motifs [3], found at P3–P1 in the signal sequence. Unusually for proteases, small peptides that mirror these protein cleavage sites have proven inefficient as substrates in SPase assays [4]. A major advance was the identification of a fusion protein, pro-OmpA–Nuclease-A, as an HPLC assay substrate efficiently cleaved by LP [1], the SPase from the Gram negative pathogen *Escherichia coli*. More recently, and concurring with our own thoughts on substrate design, the beneficial role of the membrane anchor has been demonstrated for LP with a fluorophore labelled peptide substrate [6]. However, substrates for LP have proven to be less efficient substrates for SpsB the SPase enzyme from *Staphylococcus aureus*. This Gram positive pathogen plays a significant role in infectious disease, including life threatening methicillin-resistant (MRSA) infections; so the ability to screen for, and characterise, inhibitors of SpsB would represent a significant advance for the discovery of antibacterial agents.

* Corresponding author.
E-mail address: gordon_bruton-1@gsk.com (G. Bruton).
[1] Present address: Peptide Therapeutics, Cambridge, Cambridgeshire, UK.
[2] Present address: 3607 Baldwin Hills Ct, South San Francisco, CA 94080, USA.

0223-5234/03/$ - see front matter
doi:10.1016/S0223-5234(03)00040-0

To address this situation we have used *S. aureus* genomic sequence data to design small lipopeptide substrates for SpsB, both to facilitate high throughput screening and as the basis for inhibitor design.

2. Chemistry

2.1. Design strategy

Our strategy was to incorporate the key structural features of a signal sequence into a small lipopeptide: a membrane anchor, a helix terminus or turn motif and the AXA cassette. To this end we analysed 17 *S. aureus* pre-protein sequences around the cleavage site, Fig. 1. The sequences were formatted into several broad amino acid types: (a) hydrophobic, (b) turn stabilising, (c) conformationally restricted helix-breaker or turn inducing, (d) flexible helix-breaker or turn inducing, (e) basic, and (f) acidic residues. It should be noted that asparagine, N, belongs to groups (b) and (d).

These data were reduced to a 'group' consensus sequence which, in combination with a decanoyl moiety to act as a membrane anchor and a turn inducing motif at P4–P6, formed the basis for our design of substrates **1**–**3**, Fig. 2. The final selection of residues was biased towards future compatibility with the additional moieties required for fluorescence based assays, and towards enhancing aqueous solubility where possible.

Lysine was selected for P2 to give an AKA recognition cassette and proline or asparagine for P5 due their preponderance at this position in native sequences; this being structurally significant due to their turn inducing

Gene	Residue Positions												
	P7	P6	P5	P4	P3	P2	P1	↓	P1′	P2′	P3′	P4′	P5′	P6′
EDIN	V	S	N	T	S	L	A	*	A	D	V	K	N	F
ETXB	S	T	P	N	V	L	A	*	E	S	Q	P	D	P
ETXA	T	S	P	L	V	N	G	*	S	E	K	S	E	E
HLA	M	N	P	V	A	G	A	*	A	D	S	D	I	N
SPA1	V	T	P	A	A	N	A	*	A	Q	H	D	E	A
LUKF	L	S	G	T	A	N	A	*	E	G	K	I	T	P
ETB	F	E	S	T	L	Q	A	*	K	E	Y	S	A	E
OMP7	N	N	N	E	A	S	A	*	A	A	K	P	L	D
SAK	I	T	N	E	V	S	A	*	S	S	S	F	D	K
FNBA	G	Q	D	K	E	A	A	*	A	S	E	Q	K	T
STC1	W	D	N	K	A	D	A	*	I	V	T	K	D	Y
ETA	Q	K	N	H	A	K	A	*	E	V	S	A	E	E
PHLC	T	D	N	S	A	K	A	*	E	S	K	K	D	D
LUKS	L	L	E	N	A	K	A	*	A	N	D	T	E	D
BLAC	N	S	N	S	S	H	A	*	K	E	L	N	D	L
ETXD	S	P	L	N	V	K	A	*	N	E	N	I	D	S
TSST	I	I	K	T	A	K	A	*	S	T	N	D	N	I

Fig. 1. Pre-protein cleavage site sequences from *S. aureus*. Single letter codes for amino acids with colour coded groups (a) ■ = A, V, L, I, F, W, M, Y; (b) □ = S, T, N, Q; (c) ■ = P; (d) ■ = G; (e) ■ = K, H, R; (f) ■ = D, E. Arrow indicates cleavage site.

	Residue Positions												
	P7	P6	P5	P4	P3	P2	P1	P1′	P2′	P3′	P4′	P5′	P6′
Consensus													
Alternatives													
Substrates													
1 Decanoyl-	L	T	P	T	A	K	A	A	S	K	I	D	D
2 Decanoyl-	L	T	N	T	A	K	A	A	S	K	I	D	D
3 Decanoyl-	L	T	N	T	A	K	A	E	S	K	I	D	D

Fig. 2. Consensus sequence for *S. aureus* pre-protein cleavage sites and target lipopeptides **1**, **2** and **3**. Colour coding according to Fig. 1.

properties. The remaining residues were chosen in accordance with the consensus sequence to reflect the hydrophobicity profile of signal sequences whilst enhancing the probability of a turn structure at P5. The counter intuitive choice of *iso*-leucine at P4′ was to mimic the effect of an alkyl chain tethering future fluorophore tags.

2.2. Synthetic methodology

Lipopeptides **1**–**3**, **5**–**10** and **13** were synthesised by standard solid phase chemistry on a peptide synthesiser, and purified to 95% purity or greater using reverse phase preparative HPLC. Lipopeptide α-ketoamide inhibitors **14**–**17** were similarly prepared, but with the additional incorporation of a 3-amino-2-hydroxy-butyric acid unit at P1′. For **16** and **17** this was oxidised to an α-ketoamide, using Dess-Martin periodinane [7], prior to cleavage from resin support. For **14** and **15** the terminal hydroxy-butyric acid was cleaved from the resin and coupled to 1-naphthalenemethylamine, utilising standard EDC/HOAT peptide formation procedures, prior to hydroxyl oxidation using Dess-Martin periodinane.

3. Experimental protocols

3.1. General procedures for lipopeptides *1–3, 5–10 and 13*

Lipopeptides were prepared on a peptide synthesiser using literature methodology [9] and purified to 95% or greater by reverse phase prep HPLC (Gilson; water + 0.1% TFA/MeCN + 0.1% TFA, gradient elution); purity was established using at least two analytical HPL methods and MS.

3.1.1. General oxidative procedure for α-ketoamides *16 and 17*

Resin bound lipopeptides, containing an unprotected 2-hydroxy-butanoylamino unit at P1′ (otherwise *t*-butyl protected OHs, trityl protected NH_2s), prepared by

general literature procedures [9] on WANG resin (0.0338 mmol, 61 mg), was swollen in DMF (5 × 5 mL), filtered, and suspended in DMF (1 mL). Dess-Martin periodinane reagent [7] (0.135 mmol, 0.0569 g) in DMF (2 mL) was then added under argon. The reaction was shaken for 5 h, then filtered and the resin washed with DMF (5 × 5 mL), Dioxane (5 × 5 mL), and DCM (5 × 5 mL). The resin was dried, under vacuum, over night and then treated with TFA/water (95:5) (3 mL) and agitated for 1.5 h. The resin was filtered off and the filtrate evaporated to a minimum and then co-evaporated with toluene (3 × 5 mL) to give a white powder. Purification by preparative reverse phase HPLC (Gilson; water+0.1% TFA/MeCN+0.1% TFA, gradient elution) gave lipopeptide α-ketoamides **16** and **17**. Assigned NMR for **17**: δ (methanol-d_4, 292 K); Decanoyl 2.2 (H2), 1.55 (H3), 1.26 (H4–H9), 0.87 (H10), P7 Leu 4.47 (Hα), 1.53 (Hβ), 1.66 (Hγ), 0.91 (Hδ), 0.87 (Hδ), P6 Thr 4.63 (Hα), 4.22 (Hβ), 1.35 (Hγ), P5 Pro 4.47 (Hα), 2.1 (Hβ), 2.0 (Hγ), 3.8 (Hδ), P4 Thr 4.63 (Hα), 4.12 (Hβ), 1.15 (Hγ), P3 Ala 4.26 (Hα), 1.19 (Hβ), P2 Asn 4.5 (Hα), 2.8 (Hβ), P1 Ala 4.25 (Hα), 1.15 (Hβ), P1′ βAla 3.49 (Hα), 2.46 (Hβ), P2′ Asp (Hα, masked by HOD), 2.66 (Hβ). Accurate TOF MS/MS: $[MH]^+$ 1056.56 (Calc. $[M]^+$, 1055.56).

3.2. Structural determination of *1* by NMR

NMR sample of **1** (2 mM) in 90% H_2O/10% D_2O containing 200 mM perdeuterated sodium dodecyl sulphate (SDS-d_{25}) and the pH adjusted to 4. NMR spectra were recorded at 307 K on a Bruker AVANCE 600 and proton chemical shifts referenced to 2,2-dimethyl-2-silapentane-5-suphonic acid at 0 ppm. 2D DQF-COSY, TOCSY and NOESY experiments were all acquired in the phase sensitive mode using time proportional phase incrementation and water suppression achieved using continuous pre-irradiation of the residual water signal. All processing and analysis was performed within the XWINNMR software (Bruker); NMR: δ (SDS d_{25}); Decanoyl 2.42 (H2), 2.32 (H2), 1.60 (H3), 1.29 (H4), 1.26 (H5–H9), 0.84 (H10), P7 Leu 7.99 (NH), 4.19 (Hα), 1.75 and 1.63 (Hβ), 1.73 (Hγ), 0.97 (Hδ), 0.91(Hδ), P6 Thr 8.31 (NH), 4.42 (Hα), 4.42 (Hβ), 1.25 (Hγ), P5 Pro 4.36 (Hα), 2.35 and 1.88 (Hβ), 2.10 (Hγ), 2.02 (Hγ), 3.73 (Hδ), P4 Thr 7.64 (NH), 3.99 (Hα), 4.22 (Hβ), 1.22 (Hγ), P3 Ala 8.03 (NH), 4.18 (Hα), 1.52 (Hβ), P2 Lys 7.96 (NH), 4.07 (Hα), 1.9 (Hβ), 1.56(Hγ), 1.44 (Hγ), 1.70 (Hδ), 2.97 (Hε), 7.42 (ε-NH), P1 Ala 8.14 (NH), 4.08 (Hα), 1.48 (Hβ), P1′ Ala 8.23 (NH), 4.05 (Hα), 1.48 (Hβ), P2′ Ser 7.81 (NH), 4.32 (Hα), 4.0 (Hβ), P3′ Lys 7.73 (NH), 4.29 (Hα), 1.95 (Hβ), 1.52 (Hγ), 1.72 (Hδ), 3.00(Hε), 7.42 (ε-NH), P4′ Ile 7.56 (NH), 4.12 (Hα), 1.93 (Hβ), 1.55(Hγ), 1.22 (Hγ), 0.92 (Meγ), 0.87 (Hδ), P5′ Asp 8.13 (NH), 4.78 (Hα), 2.97 and 2.81 (Hβ), P6′ Asp 7.91 (NH), 4.68 (Hα) and 2.89 (Hβ).

NMR: δ (90% methanol-d_3, 10% H_2O); Decanoyl 2.26 (H2), 2.16 (H2), 1.59 (H3), 1.27 (H4–H9), 0.87 (H10), P7 Leu 8.43 (NH), 4.4 (Hα), 1.61 (Hβ), 1.66 (Hγ), 0.94 (Hδ), 0.88(Hδ), P6 Thr 7.56 (NH), 4.68 (Hα), 4.51 (Hβ), 1.3 (Hγ), P5 Pro 4.27 (Hα), 2.39 and 2.0 (Hβ), 2.19 (Hγ), 2.05 (Hγ), 3.91 (Hδ), P4 Thr 7.71 (NH), 3.96 (Hα), 4.06 (Hβ), 1.23 (Hγ), P3 Ala 7.89 (NH), 4.12 (Hα), 1.48 (Hβ), P2 Lys 8.17 (NH), 4.0 (Hα), 1.86 (Hβ), 1.38(Hγ), 1.62 (Hγ), 1.56 (Hδ), 2.9 (Hε), P1 Ala 8.1 (NH), 4.12 (Hα), 1.47 (Hβ), P1′ Ala 8.16 (NH), 4.14 (Hα), 1.46 (Hβ), P2′ Ser 7.81 (NH), 4.28 (Hα), 3.95 and 3.94 (Hβ), P3′ Lys 7.77 (NH), 4.24 (Hα), 1.95 and 1.91 (Hβ), 1.5 (Hγ), 1.68 (Hδ), 2.94 (Hε), P4′ Ile 7.75 (NH), 4.13 (Hα), 1.88 (Hβ), 1.55(Hγ), 1.19 (Hγ), 0.92 (Meγ), 0.87 (Hδ), P5′ Asp 8.25 (NH), 4.74 (Hα), 2.90 and 2.75 (Hβ), P6′ Asp 7.91 (NH), 4.72 (Hα) and 2.85 (Hβ). MS; (ES) 1486.2 $[M+2H]^{2+}$. Amino acid analysis; D 2.2(2), S 0.9(1), T 1.8 (2), A 2.7(3), P 1.3(1), I 1.1(1), L 1.2(1), K 1.8(2).

3.2.1. Conformation modelling using NMR dihedral angles and NOE derived distance restraints

Calculations were performed using the distance geometry program DGII within the NMR-Refine module of InsightII. Distance restraints were classified into three categories with upper bounds of 2.7, 3.5 and 4.5 Å based on NOESY (150 ms) peak volumes. Pseudoatoms were used for non-resolvable methylenes and methyls and the upper bounds adjusted by 1 Å. A force constant of 10 kcal mol^{-1} was used to enforce all restraints. Calculations consisted of three steps; smoothing, embedding and optimisation. Optimisation involved simulated annealing with a maximum temperature of 1000 K and step sizes of 0.2 ps followed by energy minimisation using a conjugated gradient. From the 50 structures generated, 15 low energy structures were selected which had no distance restraint violations greater than 0.2 Å and acceptable dihedral angle restraint violations.

3.3. Assay protocols

3.3.1. Substrate cleavage by SpsB and LP

The assay protocol was similar to those described previously [9–11]: assays of SpsB and LP activity were performed in 50 mM CHES, pH 8.5, 1 mM EDTA, 0.1% Triton X-100, 0.5 mM PMSF. Enzyme, 10 nM SpsB or 20 nM LP, and substrate was incubated at 37 °C for appropriate time and reactions were quenched by addition of methanol to 50% (v/v) or addition of TFA to 0.5% (v/v) respectively. Percentage cleavage was determined by separation and quantitation of substrate and product peptides by HPLC analysis. SpsB and LP display apparent Michaelis–Menten kinetics towards the peptide substrate and specificity constants (k_{cat}/K_m) were determined by linear regression of double reciprocal plots.

Table 1
Cleavage of substrates **1**–**6** by SpsB

	Substrate	% Cleavage at			
		5 min	20 min	30 min	60 min
1	Decanoyl-LT-P-TAKA$^{\downarrow}$-A-SKIDD-OH	60	96	100	–
2	Decanoyl-LT-N-TAKA$^{\downarrow}$-A-SKIDD-OH	–	–	–	< 5
3	Decanoyl-LT-N-TAKA$^{\downarrow}$-E-SKIDD-OH	–	–	–	7
4	Pro-OmpA–NucA [a]	–	< 12	–	20
5	Octanoyl-LT-P-TQAKA$^{\downarrow}$-A-SKIDD-OH	48	91	–	99
6	Hexanoyl-LT-P-TQAKA$^{\downarrow}$-A-SKIDD-OH	22	58	–	99

[a] Cleavage sequence, FATVAQA$^{\downarrow}$ATSTKK.

3.3.2. Fluorescence assays for inhibitors

Assays of SpsB [11] activity were performed in 50 mM MOPS at pH 7.5 with 1 mM EDTA and 2 mM Triton TX-100 using black Dynex 96-well microtitre plates. Enzyme and fluorescent substrate [9], exhibiting a k_{cat}/K_m of 4.6×10^4 $M^{-1} s^{-1}$, were incubated at room temperature and cleavage was monitored continuously by the increase in fluorescence intensity using a BMG Polarstar fitted with a 485 nm excitation filter and a 520 nm emission filter. Determination of IC50 values were performed by incubating the enzyme with varying inhibitor concentrations (11 concentrations plus control) for 15 min followed by addition of substrate (100 nM). Initial rate data was fitted to a four parameter logistic equation to determine the IC50.

Table 2
Cleavage of P2 variant substrates by SpsB Dec–LTPTA–**X**–A$^{\downarrow}$ASKIDD-OH

Substrate	**X**	%Cleavage at	
		5 min	30 min
1	Lys	60	> 99
7	Arg	56	98
8	Asn	48	> 99
9	Leu	29	88
10	Asp	7	59

4. Results and discussion

4.1. Substrate cleavage

Substrates **1**–**10** were incubated with *S. aureus* SpsB at pH 8.5, aliquots were removed and analysed for cleavage by reverse phase LC/MS which confirmed that cleavage had occurred between P1 and P1′. The rates of processing identified lipopeptide **1** as an efficient substrate for SpsB, Table 1.

The rapid cleavage of lipopeptide **1** cannot be attributed to the decanoyl membrane anchor alone as **2** and **3** were poor substrates, Table 1. Conversely the conformational restrictions imposed by proline at P5 are thus shown to be pivotal for successful cleavage. However the contribution of the membrane anchor to substrate processing is evident when comparing **1** with **5** and **6**; decreasing lipid length correlates with decreasing rates of processing, though all three substrates are superior to the full length protein **4**, Table 1. Probing the significance of the P2 residue, Table 2, revealed a preference for basic residues and tolerance for a hydrophobic residue, but an acidic residue resulted in a significantly reduced rate of processing. Structural studies on SPases suggest that the side chain of the P2 residue is orientated out of the binding cleft into solvent and does not interact with the enzyme [1a]. Consequently the detrimental effects of P2 substituents are best attributed to changes in the conformational preferences of the substrate.

Table 3
Comparative efficiency of substrates with SpsB and LP

	Substrate	pH	*S. aureus* SpsB			*E. coli* LP		
			k_{cat} (s^{-1})	K_m (μM)	k_{cat}/K_m ($M^{-1} s^{-1}$)	k_{cat} (s^{-1})	K_m (μM)	k_{cat}/K_m ($M^{-1} s^{-1}$)
1	Dec–LTPTAKA$^{\downarrow}$ASKIDD	8.5	67	29	2.3×10^6	418	988	4.2×10^5
4	Pro-OmpA–Nuclease-A [5]	8.0	saturation kinetics unachievable	8.7	16	5.4×10^5	–	–
11	Y$^{(NO_2)}$FSASALA$^{\downarrow}$KIK^{Abz} [8]	8.5	0.00133	72	18.4	0.0098	144	68
12	K5L10YNO2FSASALA$^{\downarrow}$KIKAbz [6]	8.1	–	–	–	1.5	0.6	2.5×10^6

A detailed kinetic analysis was obtained for the processing of lipopeptide **1** by both SpsB and LP, Table 3. The kinetic profiles obtained for these two enzymes were found to differ, suggesting different substrate requirements. Lipopeptide **1** proved to be an excellent substrate for SpsB with a k_{cat}/K_m of 2.3×10^6 M^{-1} s^{-1} and a K_m of 29 μM, which contrasted with LP where the K_m of 988 μM would preclude the use of **1** as a suitable substrate for LP assays.

4.2. Substrate conformation

Structural studies of lipopeptide **1** indicated the presence of random conformations in an aqueous environment, versus helical conformations in membrane mimetic solvents (sodium dodecyl sulphate or trifluoromethanol), particularly between P6 and P2. This behaviour mirrors that of the native signal sequences in similar environments. The NMR data showed that a helical turn rather than a β-turn had been initiated by the P5 proline, see Fig. 3a.

Although the data could suggest that the cleavage site lies on a widening helix, Fig. 3b, the susceptible face of the scissile bond [1,2] is shielded from the active site serine on the inside surface of the helix. Thus alternative conformations with more exposed cleavage sites must be involved in the cleavage process. Such conformations are found within the NMR derived family, Fig. 3a, and are exemplified in Fig. 4.

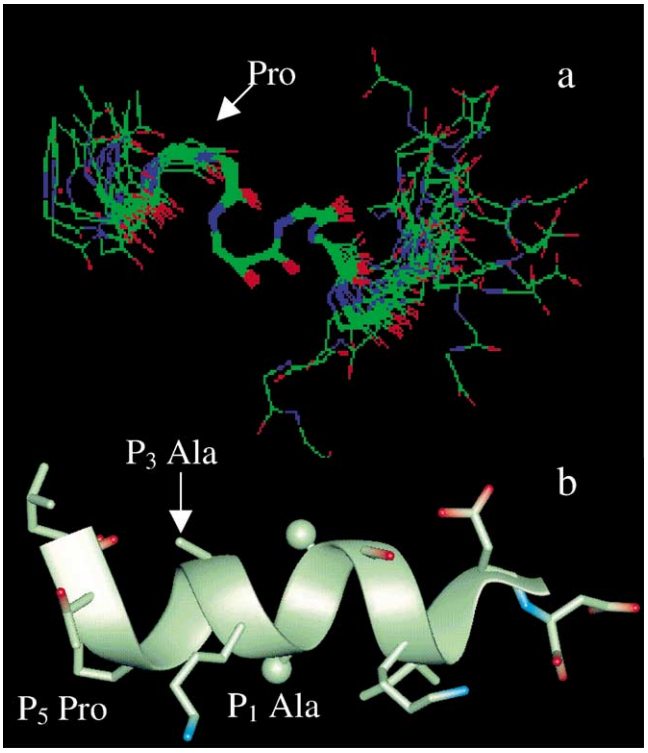

Fig. 3. (a) NMR determined structures. (b) Average NMR structure.

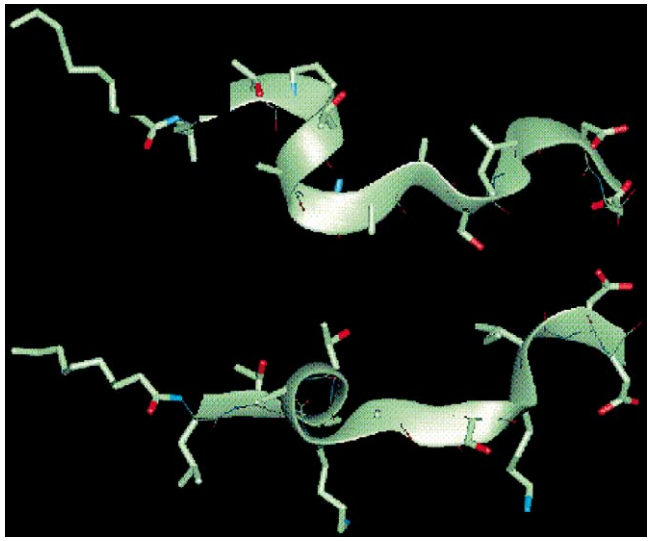

Fig. 4. Orthogonal views; an NMR determined conformation of **1** with exposed cleavage site.

Table 4
SpsB inhibitors

Decanoyl-LTPTA-**X**	SpsB Inhibition
X	IC_{50} μM
13 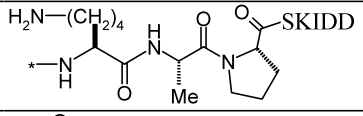	0.6
14 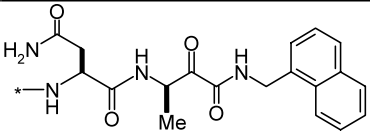	16
15 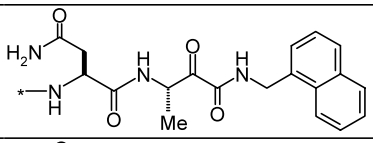	2
16 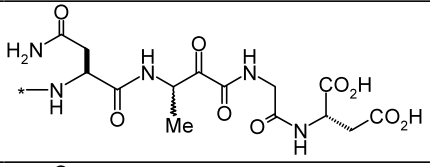	0.9
17 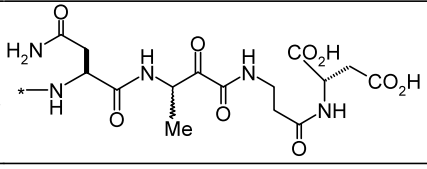	0.1

4.3. Substrate based inhibitors

Classically, either the incorporation of a proline at P1′, or the introduction of a serine trap at the cleavage site may convert serine protease substrates to inhibitors. Competitive inhibitor **13**, Table 4, confirmed that SpsB could be inhibited in this classic manner with a P1′ proline. The incorporation of α-ketoamides into **1** as serine traps is not practical, due to the incompatibility of lysine with this functionality. However the P2 lysine of **1** can be readily replaced with asparagine, see **8** Table 2, and α-ketoamide analogues **14**–**17** were found to be potent time dependant inhibitors of SpsB, Table 4. The truncated substrate analogues **16** and **17** were racemic at the P1 alanine, so their potency is underestimated in this analysis as D-alanine analogues, such as **14**, are less potent. SpsB inhibitor **17** showed no inhibition of trypsin, chymotrypsin, thermolysin or elastase at 10 $\mu g\,mL^{-1}$ (unpublished data).

5. Conclusions

We have demonstrated a successful design strategy for small, efficiently cleaved, substrates for SpsB. As a consequence SpsB is now shown to be capable of high catalytic efficiency, contrary to previous experience [4]. Combined with a membrane anchor, the conformation of peptides prior to the cleavage site is a key determinant of this cleavage efficiency by SpsB. We have also shown that SpsB is susceptible to classic protease inhibition strategies, providing that key structural features of the substrate are present.

Acknowledgements

Lesley Maclachlan and Cibele Sabido-David for their support with conformational studies, Michael Stanners for technical support and Steven Ratcliffe for contributions towards the fluorescent substrate assays.

References

[1] (a) M. Paetzel, R.E. Dalbey, N.C. Strynadka, J. Pharmacol. Ther. 87 (2000) 27–49;
(b) M. Paetzel, N.C. Strynadka, J. Prot. Sci. 8 (1999) 2533–2536.
[2] M. Black, G. Bruton, Curr. Pharm. Des. 4 (1998) 133–154.
[3] G. von Heijne, Eur. J. Biochem. 133 (1983) 19–21.
[4] N.A. Sharkov, D. Cai, J. Biol. Chem. 277 (2002) 5796–5803.
[5] S. Chatterjee, D. Suciu, R.E. Dalbey, P.C. Kahn, M. Inouye, J. Mol. Biol. 245 (1995) 311–314.
[6] R.L. Stein, D.F.S. Barbosa, R. Bruckner, Biochemistry 39 (2000) 7973–7983.
[7] R.K. Boeckman, P. Shao, J. Mullins, J. Org. Syn. 77 (2000) 141–152.
[8] W. Zhong, S.J. Benkovic, Anal. Biochem. 255 (1998) 66–73.
[9] S. Ashman, M.T. Black, G. Bruton, A.J. Humphries, K.J.M. Moore, PCT Int. Appl. (2000) WO 0046250.
[10] A.E. Allsop, G. Brooks, G. Bruton, S. Coulton, P.D. Edwards, I.K. Hatton, A.C. Kaura, S.D. McLean, N.D. Pearson, T. Smale, R. Southgate, Bioorg. Med. Chem. Lett. 5 (1995) 443.
[11] K.M. Cregg, E.I. Wilding, M.T. Black, J. Bacteriol. 178 (1996) 5712.